



International Congress of Science and Technology of Metallurgy and Materials, SAM –
CONAMET 2014

Thermal cycles and residual stresses in FSW of aluminum alloys: experimental measurements and numerical models

Luciano Buglioni^a, Leonardo N. Tufaro^a, Hernán G. Svoboda^{b,c,*}

^a*Instituto Nacional de Tecnología Industrial, Centro de Investigación y Desarrollo en Mecánica, Av. Gral Paz 5445, B1650KNA, San Martín, Buenos Aires, Argentina*

^b*Universidad de Buenos Aires, INTECIN, Facultad de Ingeniería, Laboratorio de Materiales y Estructuras, GTSyCM², Av. Las Heras 2214, C1127AAR, Ciudad Autónoma de Buenos Aires, Argentina*

^c*Consejo Nacional de Investigaciones Científicas y Técnicas (CONICET), Av. Rivadavia 1917, C1033AAJ, Ciudad Autónoma de Buenos Aires, Argentina*

Abstract

In the present work longitudinal residual stresses obtained by different methods, numerical and experimental, in Friction Stir Welding (FSW) process for AA7075 were analyzed. The experimental method employed for residual stresses measurements was sectioning, whereas the numerical is a finite element (FEM) thermomechanical coupled model which does not consider the stir in the material. The effect of travel speed during FSW was also analyzed, measuring with strain gages positioned in several points at different distances from weld centerline. From the obtained residual strains, the stress values, stress variation against weld centerline distance and null stress point were calculated. Numerical and experimental stress values agree in order of magnitude, being greater in numerical method inside stir zone's edge and even outside, and smaller at some point towards the end of plate. Stress variation against weld centerline distance and null stress position vary in different ways for each method. This phenomenon agrees with another works, and it could be related with no consideration of the stir process in the numerical method. Thus, it has been developed a simplified finite element model which averages in magnitude experimental residual stress in FSW.

© 2015 The Authors. Published by Elsevier Ltd. This is an open access article under the CC BY-NC-ND license (<http://creativecommons.org/licenses/by-nc-nd/4.0/>).

Peer-review under responsibility of the Scientific Committee of SAM–CONAMET 2014

Keywords: Residual Stresses; Friction Stir Welding (FSW); Finite Element Method (FEM); AA7075.

* Corresponding author. Tel.: +5411-4514-3009; fax: +5411-4514-3009 .
E-mail address: hsvobod@fi.uba.ar

1. Introduction

Friction stir welding (FSW) has been a technology of strong development in recent years. The introduction of this process has revolutionized the construction of welded aluminum alloy structures with many applications in industries such as aviation, aerospace, automotive and shipbuilding, among other.

The thermal cycle induced in the material during welding is an issue of great importance, because it affects aspects like plastic flow, microstructural evolution and others such as residual stresses. In particular, residual stresses present in welded components can produce beneficial or detrimental effects on the performance of those components, and have a strong influence on failure mechanisms as brittle fracture, fatigue and stress corrosion cracking [Masubuchi (1980)], which motivates their study. In this sense, studies have been made from experimental and/or numerical standpoint in order to reach better understanding of the effect of the FSW process and its variables on residual stresses.

It has been found that residual stresses present in joints welded by FSW usually have a distribution in form of "M" and that longitudinal stresses are higher than transverse ones. Although this distribution is almost symmetrical, the stresses are usually slightly higher in the AS. Regarding the influence of welding variables, it has been reported that the longitudinal stresses increase with the travel speed, whereas there are different opinions about the effect of rotation speed on the residual stresses [Masubuchi (1980), Tufaro (2012)]. Different authors [Peel et al. (2003), Woo et al. (2005)], have been encountered that for certain plate thickness and tool geometry, the effect of the tool pin (stir process) in longitudinal strains is not critical. They conclude that the heat input from the tool shoulder is a major source of the internal strains (and thus residual stresses). Nevertheless Mishra (2007) reports that the fact of adding a superimposed torque and axial force (i.e. adding the contact of a tool and the stirring effect) to a numerical model with thermal input only, leads to a reduction of resulting longitudinal stresses. It is not analyzed however in which zone this reduction occurs. Thus, it is of interest to compare this numerical observation with the experimental one referring to the small effect of stirring in residual stress occurrence.

Numerical models are a powerful tool for understanding the acting phenomena during FSW. Thermal cycle analysis can be approached either by purely thermal models or by thermo-mechanical coupled ones. These coupled models can also be used to calculate the residual stresses generated by the action of thermal and plastic deformations via thermal input. There are intermediate models that consider the contact condition at the tool-specimen, mostly the friction contribution limiting material flow by symmetry [Chen and Kovacevic (2000)]. Furthermore, some authors have proposed simpler models, considering only the heat flow contribution with a defined power density, so that the residual stresses obtained are produced exclusively by thermal effects [Khandar et al. (2006)]. Finally, there are more complex works which obtain residual stresses via two main steps. The first is to model the pseudo-transient phenomenon by thermal or complex viscoplastic models. These models are represented either by Fluid Dynamics [Bastier et al. (2008)] or by thermal [Buffa et al. (2011)] or thermo-plastic finite element formulations in different eulerian-lagrangian schemes [Al-Badour (2013), Grujicic et al. (2009), Shi et al. (2003), Zhang, Zhang (2009)]. The results, either thermal or both thermal and plastic, obtained from these models are transferred to a simpler elastoplastic or viscoelastoplastic finite element model which solves the residual stresses.

The objective of this study was to analyze the thermal cycles produced during the welding of AA70705-T651 plates by FSW and the resulting residual stresses, for different travel speeds, by experimental measurements and numerical models. In this study was implemented a numerical model which involves a thermal input, not including tool stirring effect. The advantages of this choice are at first place the drastic reduction of calculation time related to solve the mechanical plastic flow, since the tool pin is not modelled, hence the resulting plastic flow remains associated to thermal distortion only. These small plastic strains can be modelled with a single lagrangian reference, instead a more complex eulerian or eulerian-lagrangian formulations, which are used for avoid severe distortions of the mesh modelling greater plastic flow induced by the tool. Another advantage resulting from avoiding tool modelling is the fact of not consider tool-workpiece contact, which requires an important amount of computational time. On the other hand, disadvantages of the thermal approach include the unknowing of material flow due to the tool action, even the defect formations. Another one is that the contact model solves the vertical reaction of the backing plate, which can be measured and used to calibrate this model.

Nomenclature

AS	Advancing side
FEM	Finite Element Method
FSW	Friction Stir Welding
HAZ	Heat Affected Zone
h_c	Convection coefficient
NSP	Null Stress Point, Transverse Position where Longitudinal Residual Stress is Null
Q	Power of Heat Source
SG	Strain Gage
SZ	Stir Zone
σ_i	Longitudinal Residual Stress in the Position of Strain Gage “i”
T_0	Ambient Temperature
TCi	Thermocouple number “i”
U	Travel Speed
WCL	Weld Centerline
ω	Rotational Speed
x	Longitudinal Position (distance from the plate edge)
y	Transverse Position (distance from the weld centerline)
y_i	Transverse Position of Strain Gage “i”
z	Through Thickness Position (distance from the upper surface)

2. Materials and Methods*2.1. Experimental Procedure*

In order to achieve the proposed objectives, AA7075-T651 plates of 150x75x4 mm were butt welded by the FSW using an adapted milling machine. The travel speed was varied from 51 to 206 mm/min, while a rotation speed of 514 rpm and a tilt angle of 2° were used for the all joints. The FSW tool used was made of H13 tool steel, presenting a concave shoulder and a smooth tapered pin. Shoulder diameter was 12 mm, while the major and minor pin diameters were 4 and 3 mm, respectively. Finally, the pin height was 3.8 mm [Tufaro (2012)]. In Fig. 1, FSW experimental set up and a welded joint are shown.

During welding, the thermal cycles were acquired using three K-type thermocouples, which were located in the middle length of the specimen, in the retreating side. They were positioned approximately at 7, 13 and 19 mm from the weld centerline, placing them in holes with 1 mm in diameter and 2 mm deep.



Fig. 1. FSW experimental set up and a welded joint.

The sectioning method was used for the measurement of longitudinal residual stresses [Masubuchi (1980)]. For each specimen, four linear strain gages (SG) were instrumented and located in their mid-length in the advancing side with a direction parallel to the weld bead. These SG have a grid of 19 mm long and 1.6 mm wide, while the support width was 6 mm. The first SG was positioned over the center of the weld bead and the others, one after the other. The resulting transverse position of the SG (y_i) was the distance between the weld bead center and the grid center. The two cuts transverse to the weld bead which separated the portion of the specimen that contain the four SG, were performed using a horizontal milling machine with a disk cutter of 1 mm thickness. Considering the aging time effect on the mechanical properties of welded joints by FSW of age-hardenable aluminum alloys, these measurements were performed at approximately 33 days after the welding, with the aim of eliminating this variable [Tufaro (2012)].

2.2. Numerical Model

In order to obtain the residual stresses values, a three-dimensional thermo-mechanical coupled model in ANSYS® was developed. It consists of a 10548 nodes mesh and 1450 parabolic elements of 20 nodes. Each one of these nodes has 4 degrees of freedom corresponding to the displacements in the three dimensions and temperature. It is not considered the contact between the tool and the plate, so that the heat input was purely thermal.

The model is transient and it was used for all cases a 300 seconds time to allow the cooling of the plate. It was considered a bilinear material with an isotropic hardening of 1%, with temperature dependent Young modulus and yield stress [Mitchell (2014); ASM International (1992)], while the remaining material thermal parameters were remained as constant [Tufaro (2012)]. Finally, the thermal expansion coefficient was 2.52×10^{-5} m/m-C [ASM International (1992)].

A spatial distribution of the heat source linearly with the distance from its center was used for performing the model. This is because the density of heat generated by friction between the shoulder of the tool and the plates increases with the tangential velocity, which is the product of the rotational speed and distance from the center of the heat source [Schmidt and Hattel (2008); Gallais et al. (2008)]. Furthermore, it is understood that the heat is generated mainly by the interaction between the tool shoulder and the plate, so that the effect of the pin is neglected. However, this effect is considered to be of 2% to 20% or even greater [Mishra and Mahoney (2007); Nandan (2008)]. In this work, the effect of the pin was not considered in order not to complicate numerical model.

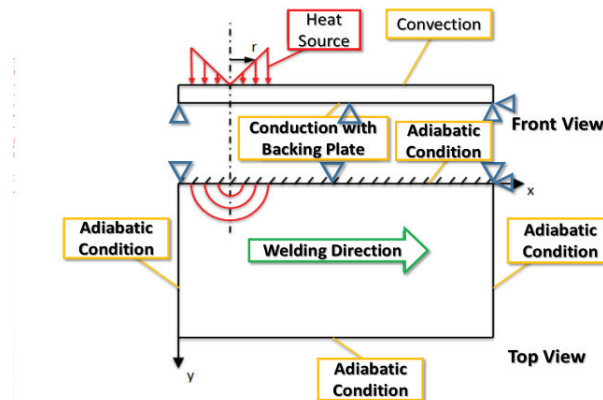


Fig. 2. Schematic diagram of numerical model.

Heat losses into the environment by conduction to the backing plate and by convection on the upper and lower surfaces of the plate were taken into account, while lateral convection was not considered. Since the problem was considered symmetric respect to the weld centerline, which coincides with the x axis, the model may be resolved by considering only the half of the original domain with an adiabatic border condition on the symmetry line. In Fig. 2

the front and top views of the domain are represented showing the heat source, the thermal and mechanical border conditions, and the coordinate axes used to define the problem.

It can be seen that displacement restrictions were applied on the bottom surface of the plate for vertical displacement restriction, whereas the weld centerline was fixed because of the symmetry condition. On the other hand, the outer edge of the plate was not restricted in the model whereas it was restricted indeed in the FSW experimental set up. A test model was performed in which this boundary was fixed, releasing it at the end of the process. It was observed that the transverse displacements due to thermal deformation during the process were in inward direction (into the weld centerline), and these fixings restricted them, which actually resulted in a not physical condition (since the fixings only restrict displacements in outward direction) and a large increase in stress. Also, in the process were observed small displacements in the transverse direction. For these reasons, these restrictions were released and the vertical displacement related of the clamping system and its subsequent release, were avoided. Finally, the plate was not restricted longitudinally since one edge is free in the FSW experimental set up.

The heat dissipated by convection depends on the convection coefficient (h_c) between the plate edge and the ambient, which is considered $20 \text{ W(m}^2\text{K)}^{-1}$ [Mishra and Mahoney (2007)]. Moreover, it is assumed that the heat transfer to the plate was with a large solid which was at constant ambient temperature (T_0). The heat dissipated by conduction depends on the conduction coefficient (h_k), although it can be estimated, it was an unknown parameter which is determined experimentally by adjusting the maximum temperature at the hottest thermocouple (TC1) for different values of this coefficient. Then it was taken a value of $200 \text{ W(m}^2\text{K)}^{-1}$, which showed a lower error in the cooling curves for the different analyzed feed rates.

In order to obtain the residual stress from the numerical model it must be given an input value of the power (Q) for each travel speed. These values of power were obtained from a purely thermal numerical model developed in previous work [Tufaro (2012)] and by matching the experimental thermal cycles of the hottest thermocouple TC1. Once obtained these values of power, an adjusting expression depending on the travel speed was obtained, and then applied as a heat flow in this thermo-mechanical model whose parameters (material, conduction to the backing plate, convection) were similar.

3. Results and Discussion

3.1. Thermal Cycles

Fig. 3 shows the comparison between the experimental thermal cycles and those obtained numerically from the thermo-mechanical model, for different values of U .

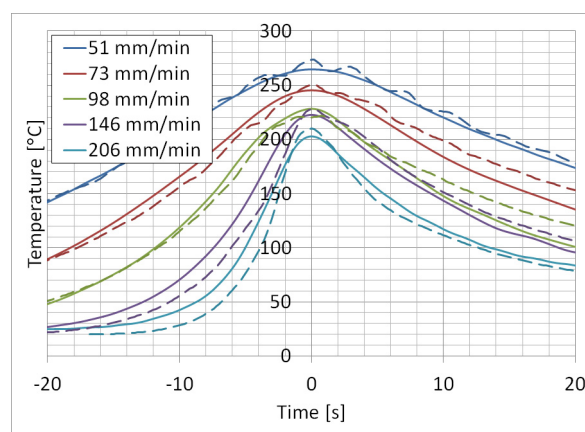


Fig. 3. Thermal cycles obtained by experimental measurements (solid line) and numerical model (dotted line) corresponding to the TC1 for different travel speeds.

It is observed that although the powers were fitted with the thermal model described above, the results are acceptable. The oscillations in the thermal cycles may be due to the parabolic nature of the elements. Although the small variations in the location of the TC1 for each welding condition, the decreasing of the peak temperature and the raising of the cooling rate by increasing the travel speed (U) are observed.

3.2. Residual Stresses

Longitudinal residual stresses were obtained from different strain gages placed in the mid-length ($x = 75$ mm) and in the top surface ($z = 4$ mm) of the plate in different transverse positions (y_i) as shown in Table 1. The small variations in the transverse position of the strain gages (y_i) are associated with the experimental technique used to place them.

Table 1. Distance to the weld centerline of strain gages for the five analyzed welding conditions.

U (mm/min)	y_A (mm)	y_B (mm)	y_C (mm)	y_D (mm)
51	0	6	12	18
73	0	6	12.5	19
98	0	6.5	13.5	19.5
146	0	7	13	-
206	0	6.5	13	19

Table 2 shows the results obtained by both methods described in the above points. It should be noted that the strain gages measure the strain from a non-point grid, so that the values obtained correspond to an average of the strain of the effective zone of the strain gage. It is also indicated in table the power (Q) entered to the numerical model and the transverse position where the residual stress is null (NSP). It can be seen that the values of residual stress are in the same order of magnitude for both methods.

Table 2. Longitudinal residual stresses obtained by different methods and other calculated parameters.

Method	U (m/min)	Q (W)	σ_A (MPa)	σ_B (MPa)	σ_C (MPa)	σ_D (MPa)	NSP (mm)
Experimental	51	-	53	37	7	-11	15.8
	73	-	63	50	25	8	21.1
	98	-	73	58	30	10	22.0
	146	-	72	51	22	-	17.6
	206	-	78	49	22	11	21.8
Numerical	51	387	87	89	-4	-2	11.7
	73	393	92	96	-18	-19	11.5
	98	400	93	81	-21	-16	10.1
	146	412	109	86	-25	-	10.5
	206	428	130	68	-19	-14	8.3

The values of longitudinal residual stress obtained by the experimental method are plotted in Fig. 4 for the five analyzed travel speeds. It is shown that the stress variation from the weld centerline to the plate edge is approximately uniform. Also, it can be seen that the residual stresses are increased with U for low travel speeds, while these do not significantly vary at high speeds (146mm / min, 206 mm / min) [Tufaro (2012)]. It is interesting to note that according to [Peel et al. (2003)], although measured peak longitudinal stresses increase as U increases, tensile stresses appear to be limited to the softened weld zone instead, resulting in a narrowing of the tensile region. According to Chen and Kovacevic (2000), measured peak stresses also increase, however this narrowing effect is

not observed (NSP remains the same). On the other hand, these authors report experimental longitudinal stress gradients which are both in agreement with results in Fig. 4 (around 5MPa/mm).

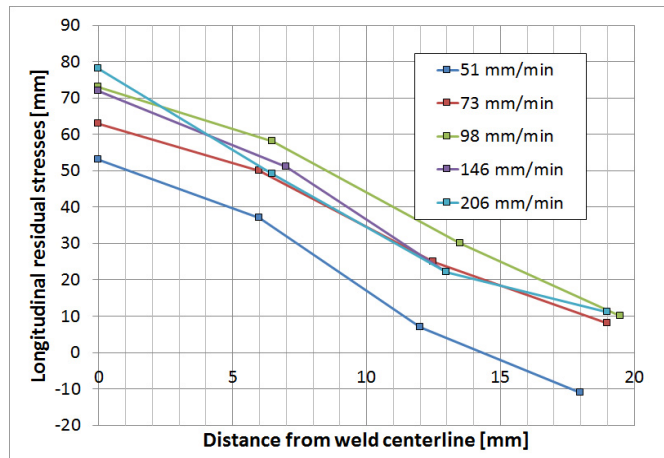


Fig. 4. Longitudinal residual stresses obtained by experimental measurements for different travel speeds (U).

The values of longitudinal residual stress obtained by the numerical method are shown in Fig. 5. The stress gradient in the transverse direction becomes more pronounced with the increase of U. Maximum stress values within the stir zone (where the model is less representative because it not considers the material flow) are also increased with increasing travel speed. These two features are consistent with works of other authors that consider friction [Chen and Kovacevic (2000)]. However, it has been seen that the residual stress decreases with the increasing of U outside the stir zone from about 7 mm of the weld bead edge.

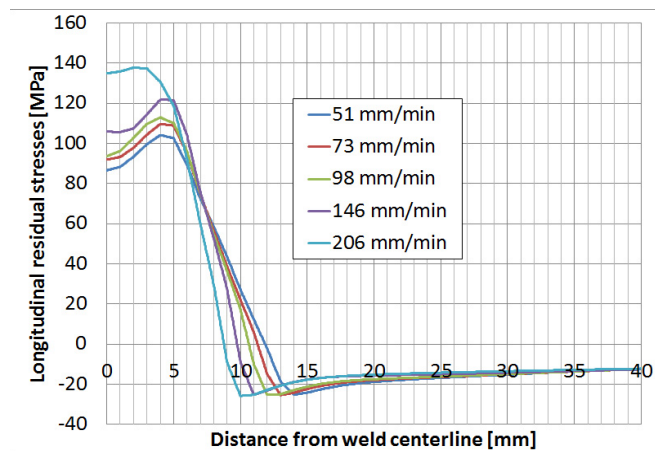


Fig. 5. Longitudinal residual stresses obtained by numerical model for different travel speeds (U).

Fig. 6 shows a graph comparing the residual stresses corresponding to the extreme speeds (51 and 206 mm/min) obtained by both methods. It can be seen that the experimental case has a lower stress variation from the weld centerline to the plate edge than the numerical case. This greater stress uniformity in the first case may be induced by the plastic deformation due to the tool stirring action and also may be influenced by the dimensions of the strain gage, as mentioned above.

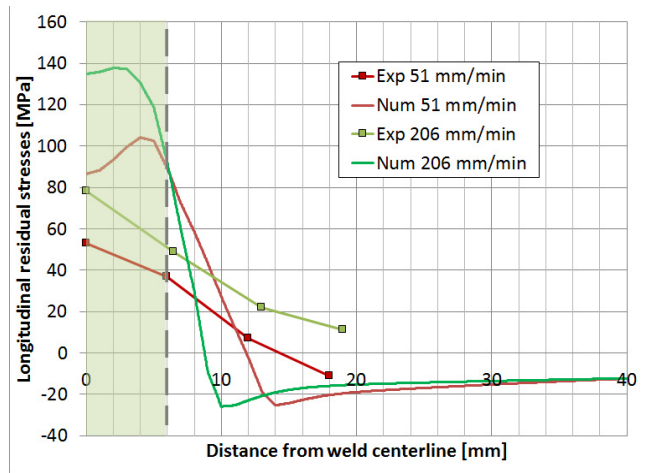


Fig. 6. Longitudinal residual stresses obtained by both methods for 51 and 206 mm/min.

Inside the stirring zone, it is seen that the stresses increase with U for both methods. The fact that the numerical model show higher residual stresses that the experimental one agrees with works of other authors [Chen and Kovacevic (2000), Khandar et al. (2006)] and may be due to the tool stirring action decreases the stress in this zone.

In the numerical case, the stress variation in the heat affected zone (HAZ) is more pronounced than in the experimental measurement, consistent with other studies [Chen and Kovacevic (2000), Khandar et al. (2006)]. The fact that numerical residual stresses are greater in the stirred zone causes an abrupt variation of stresses associated with the balance in this direction. When considering the friction, the contact of the tool and the plastic flow; the stresses within the stirring zone decrease [Mishra and Mahoney (2007)] and thus would result in a less pronounced variation of these stresses, with a shift of the null stress point (NSP).

Correlations for the null stress point (NSP) with U for the experimental and numerical cases are shown in Fig. 7. It is seen that in the experimental case the null tension point is further away from the center of the weld bead. It has been reported in literature [Shi et al. (2003), Mishra and Mahoney (2007)] that by including vertical force, the contact shoulder of the tool and torque imposed by this in a numerical model, the NSP moves away of the weld bead. This aspect and the fact that the stresses within the heat input zone decrease in this model would both explain the observed differences between the two residual stress profiles obtained for each method.

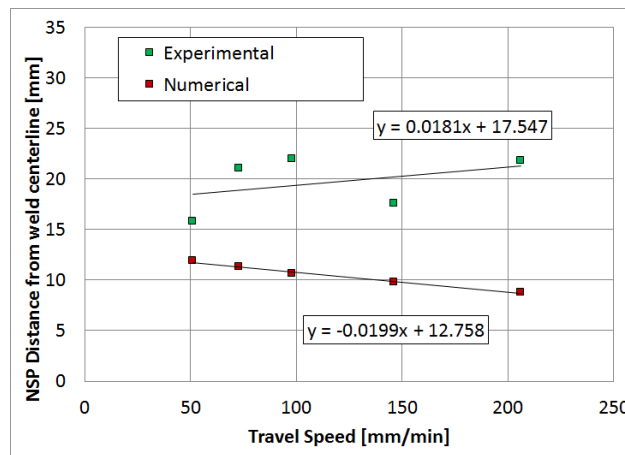


Fig. 7. NSP obtained for both methods vs. U.

In both cases the variation of NSP has a little dependency with U. In the numerical case this point narrows the weld bead with the increase of the travel speed, while in the experimental model it is observed that the NSP tends to move away from the weld. It has not seen a significant variation of this point in works of other authors [Chen and Kovacevic (2000)].

The residual stresses and the plastic deformations obtained from the numerical model, both in the longitudinal direction, are shown in Fig. 8 for 51 and 206 mm /min.

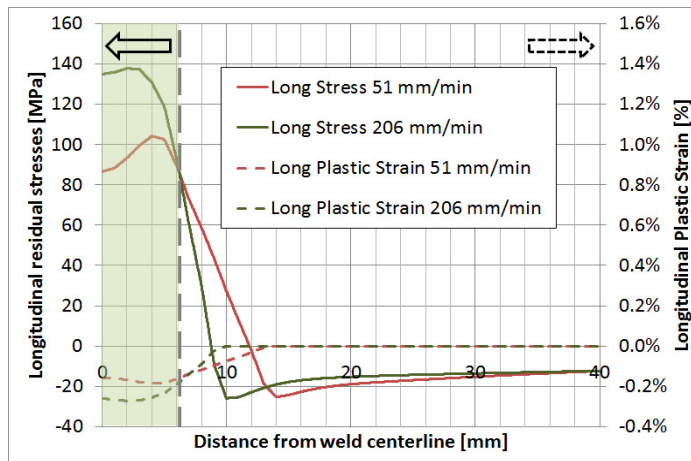


Fig. 8. Longitudinal residual stresses and longitudinal plastic deformation for 51 and 206 mm/min.

It can be seen that the deformations for the lower travel speed (red line) are smaller in magnitude than the deformations obtained for the faster travel speed (green line) within the stir zone. The same aspect applies to the residual stresses in this zone. However, beyond the SZ, the values of residual stresses and plastic deformations become smaller in magnitude for the faster travel speeds. A match between changes in deformations and the residual stresses profile is verified.

In future works, in order to complement the results obtained in this work the vertical restriction and subsequent clamps releases will be analyzed. It is also of interest to consider the variation of the thermal expansion coefficient with temperature, and the influence of a kinematic hardening, even the influence of different values of this hardening. In turn, it is of interest to develop a numerical model of friction restricting the displacement in the symmetry line and imposing a mechanical source to replace the current heat source, in order to analyze the impact of the vertical force of the tool. Another future task can be to consider an alternative numerical material constitutive law, like elastoviscoplastic Johnson-Cook [Al-Badour (2013), Zhang, Zhang (2008), Grujicic et al. (2009)] material. This material model can be conjugated either with the thermal input model developed in this work or with a contact model accounting for tool stirring effect, achieved with a single mesh representing both welded probes. Another analysis can include a Fluid Dynamics approach.

4. Conclusions

In the present work were developed both experimental and numerical approaches, in order to obtain residual stresses in FSW processes. The obtained values have been correlated, from both ways considering the analysis zones. In stir zone and its narrowing the resulting stresses from numerical model are greater than experimental ones, which can be explained by the fact that numerical model is not considering stirring effect. In HAZ zone measured residual stresses are in agreement with those calculated, with a peak of 80MPa. Numerical model predicts a greater longitudinal stress gradient than measured value. Tensile zone, related to NSP is greater in experimental case, extending to 20 mm, whereas numerical model reaches to an average of 10 mm. Experimental longitudinal stresses increase with travel speed until certain value, whereas in numerical model was observed an increase of gradient with

travel speed. It was verified a correlation between residual stresses and plastic strain calculated both in longitudinal direction. In this work was developed a numerical tool which approaches in magnitude longitudinal residual stresses in FSW processes, with some differences according to limitations and simplifications adopted.

Acknowledgements

The authors want to acknowledge to INTI and Universidad de Buenos Aires for the financial support for this work and to the personnel of the Laboratorio de Materiales y Estructuras - FIUBA and INTI-Mecánica for its collaboration.

References

- Al-Badour F., Merah N., Shuaib A., Bazoune A., 2013. Coupled Eulerian Lagrangian finite element modeling of friction stir welding processes. *Journal of Materials Processing Technology*, 1433-1439.
- ASM Handbook, Properties and Selection: Nonferrous Alloys and Special-Purpose Materials, vol. 2. Ohio: ASM International, 2002.
- Bastier A., Maitournam M.H., Roger F., Dang Van K., 2008. Modelling of the residual state of friction stir welded plates. *Journal of Materials Processing Technology*, 25-37.
- Buffa, G., Ducato, A., Fratini, L., 2011. Numerical procedure for residual stresses prediction in friction stir welding. *Finite Elements in Analysis and Design* 47, 470–476.
- Chen, C.M., Kovacevic R., 2000. Finite element modeling of friction stir welding—thermal and thermomechanical analysis. *International Journal of Machine Tools & Manufacture* 43, 1319–1326.
- Gallais, G. C., Denquin A., Bréchet Y., Lapasset G., 2008. Precipitation microstructures in an AA6056 aluminium alloy after friction stir welding: Characterisation and modelling. *Materials Science and Engineering*, 496, 77–496.
- Grujicic M., He T., Akaere G., Yalavarthy, H.V., Yen C-F., Cheeseman B.A., 2010. Fully coupled thermomechanical finite element analysis of material evolution during friction-stir welding of AA5083. *Journal of Engineering Manufacture* 224, 609-625.
- Khandar, M. Z. H., Khan, J. A., Reynolds, A. P., Sutton, M. A., 2006. Predicting residual thermal stresses in friction stir welded metals. *Journal of Materials Processing Technology* 174, 195–203.
- Masubuchi, K., 1980. *Analysis of Welded Structures - Residual Stresses, Distortion, and their Consequences*. New York, Pergamon Press.
- Mishra, R. S., Mahoney, M. W., 2007. *Friction Stir Welding and Processing*. ASM Internacional.
- Mitchell, I., 2004. *Residual Stress Reduction During Quenching of Wrought 7075 Aluminum Alloy*. Worcester: Worcester Polytechnic Institute.
- Nandan, R., DebRoy, T., Bhadeshia, H. K. D. H., 2008. Recent advances in friction-stir welding - Process, weldment structure and properties. *Progress in Materials Science* 53, 980-1023.
- Peel M., Steuwer A., Preuss M., P.J. Withers, 2003. Microstructure, mechanical properties and residual stresses as a function of welding speed in aluminium AA5083 friction stir welds. *Acta Materialia* 51, 4791-4801.
- Schmidt, H. B., Hattel, J. H., 2008. Thermal modelling of friction stir welding. *Scripta Materialia* 58, 332–337.
- Shi, Q.Y., Dickerson, T., Shercliff, H.R.. *Thermomechanical FE Modeling of Friction Stir Welding*, 2003. Proc. Fourth Int. Symp. on Friction Stir Welding, Park City, UT, TWI.
- Tufaro, L. N., 2012. Tensiones residuales y propiedades mecánicas de uniones soldadas por fricción agitación (FSW) de AA 7075-T651, Facultad de Ingeniería, Universidad de Buenos Aires.
- Woo W., Choo H., Brown D.W., Bourke M.A.M., Feng Z., David S.A., Hubbard C.R., Liaw P.K., 2005. Deconvoluting the influences of heat and plastic deformation on internal strains generated by friction stir processing. *Applied Physics Letters* 86, 231902.
- Zhang Z., Zhang H.W., 2009. *Journal of Materials Processing Technology* 209, 241-270.